A Heat and Mass Transfer Study—Analysis of Continuous Processes for the Coloration of Polyester Fabric. I. Heat Transmission to the Fabric System—Fabric, Fiber, and Dye Particles

SAMI E. AKAOUI,* *School of Textiles, North Carolina State University, Raleigh, North Carolina 27650*

Synopsis

The three continuous processes (thermosol, high temperature steaming, and heat transfer printing) for the coloration of polyester and the involved equipment are briefly reviewed. A simple model for the transient heating of a body is developed, the model [eq. (22)] comprises a specific area of transfer parameter (A_s): area through which transport (of heat) takes place per unit mass of the body. This model is used in order to estimate the relative heating rates for the different geometrical approximations present in the fabric system: plate (fabric), cylinder (fiber), and sphere (dye particle). Results obtained from the more exact numerical analysis solution are used for investigating the limitations of the simple heat transfer model.

INTRODUCTION

This study investigates three standard processes for coloring polyester with disperse dyes: thermosol, high temperature steaming (HT steaming), and the conventional heat transfer printing (HTP). In the first part of this process examination, the heat transfer to the fabric system (fabric, fiber, and dye particle) is analyzed in order to determine the relative heating rate of each component in the fabric system, and the consequent limitations on the possible heat transfer coefficient, and the heat source temperature for heating the fabric to a certain temperature in the heating unit. At the end of Paper I, a comparison is made between results obtained from the simple model [eq. (22)] used for the above—and commonly used in different forms in the textile literature—and results from the more accurate numerical analysis. Paper II of the enquiry compares the heating characteristics of the three coloration processes. Results obtained from both Papers I and II are utilized in Paper III for the modelling of the simultaneous heat and mass transport involved in the three coloration processes, and a comparative efficiency analysis is finally made with recommendations on what more direct coloration processes should involve in terms of operation and process variables.

CURRENT CONTINUOUS PROCESSES FOR COLORING POLYESTER WITH DISPERSE DYES

Presently there are three major processes for continuously coloring polyester fabric with disperse dyes: thermosol, high temperature steaming (HT Steaming),

* Candidate for Ph.D. degree in Fiber and Polymer Science.

Journal of Applied Polymer Science, Vol. 27, 4693–4711 (1982)

CCC 0021-8995/82/124693-19$02.90

and heat transfer printing (HTP). According to the most recent statistics from *Textile Machinery Trends* (1977–78), the total number of Thermosol-Pad and Steam Ranges in the United States is 132, and the number of HTP units in place is 77 with 59 continuous process units. In 1977, the output of polyester fibers dyed and printed amounted to approximately 4 million tons (worldwide) consuming 400,000 kg of disperse dyes every day.[1]

Polyester fiber [poly(ethylene terephthalate) (PET)] offered considerable difficulties in dyeing when it was first produced by the Imperial Chemical Industries (ICI) as Terylene® in 1947. The polymer PET was discovered in 1941 by J. R. Whinfield and J. T. Dickson in England. Due to the lack of hydrophilic properties, PET fibers have no affinity for water-soluble dyes like, say, direct dyes that are used to dye cotton. Furthermore, polyester has no reactive groups such as those present in cellulose (hydroxy groups) and protein (amino groups) fibers. Only one major class of dyestuff proved to be practical for dyeing unmodified polyester: disperse dyes—a nonionic dye class. Disperse dyes were discovered by Ellis in 1920 and were used for dyeing cellulose acetate. Presently, disperse dyes are used for coloring cellulose acetate, nylon, polyester, and acrylic fibers.

Several classes of processes have been developed to overcome the difficulties of dyeing polyester with disperse dyes, viz., aqueous dyeing under atmospheric conditions, pressure dyeing, carrier dyeing, and vapor phase coloration, as in thermosol, HT steaming, and HTP. The vapor phase coloration processes can be operated continuously and are carried out at high temperatures at around 200°C for residence times varying from 1 min to 20 s—as in HTP. The former (aqueous) processes are batch, and the dyeing takes place at about 100°C for 1 h or more, except for pressure dyeing where the operating temperature can be as high as 140°C and the residence time is less than an hour—around 30 min.

Relatively speaking, better quality control can be achieved in continuous (steady state) coloration processes whereas batch processing of the material involves transient conditions that make larger quantities of textile goods more difficult to control; this makes the continuous coloration processes of large quantities of polyester material more economical.

Thermosol

Thermosol is a process for fixing—immobilizing—disperse dyes in polyester fiber using air as the heating medium. This process was introduced by the DuPont Co. in the early 1950s.[2] A typical sequence of operations for continuously dyeing (or printing) polyester fibers involves padding the polyester fabric with a disperse dye solution, drying the fabric, and then driving the dry fabric into a hot air oven at the desired temperature (around 200°C) for a predetermined residence time that varies from 60 to 90 s, depending on the required shade depth, specific weight of fabric, and equipent used.[3] Pale (pastel) shades and light fabrics need less fixation time then deep (dark) shades and heavy fabrics. This process became particularly successful in the United States; its commercial implementation took place in the late 1950s; 1.0–1.2 m/s are normally produced using thermosol units.[3]

There are four major types of Thermosol units: (1) units based on forced convection of hot air through the fabric; (2) direct contact units in which the

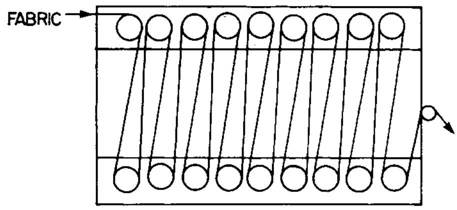

Fig. 1. Hot flue thermosol unit.

fabric is passed between heated cylinders; (3) conduction–convection units whereby the fabric is driven through perforated heated cylinders that allow simultaneous forced convection and conduction to take place; and (4) infrared radiation units.

Forced convection units fall into two categories. (a) Hot flue units (Fig. 1): The fabric is entered in its full width into the heating chamber and driven through a fringed path; thereby a large amount of fabric is processed per unit length of the equipment. These units require a long thread up and are frequently used for high speed production; 1.5–2.3 m/s.[4] (b) Tenter frame units (Fig. 2): Both edges of the fabric are clipped by two endless chains that guide the fabric horizontally into this thermosol unit, and hot air is blown on both sides of the fabric [Fig. 2(a)] during its straight path. Of course, such units have a lower fabric capacity and occupy more floor space than the hot flue units; however, the heating efficiency, because of full fabric exposure to heating medium, is almost 10 times higher.[5]

Direct contact units have different modes of heating the fabric (see Fig. 3) that vary from directly heating the interior of the cylinder by burning a fuel and

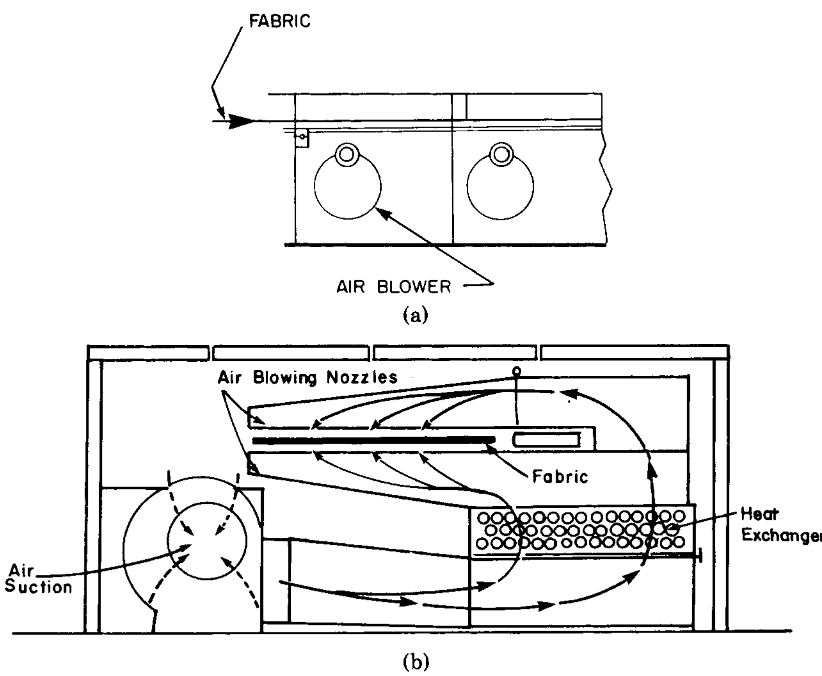

Fig. 2. (a) Tenter frame thermosol unit; (b) air path in tenter frame of unit shown in (a).

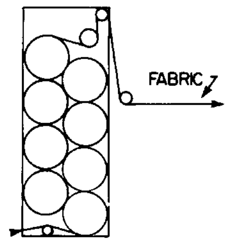

Fig. 3. Direct contact thermosol unit.

producing a flame inside the cylinder (gas-fired units) or heating the cylinders by continuously circulating steam, or other heating media inside the cylinder. These directly heated "cans" have a shorter thread-up length and occupy less space than common hot air convection units, but they require a long heating time for startup. Heavy shades of dyed fabric can be produced using heated cans at a rate of 0.6–0.9 m/s.[6] Figure 4 illustrates a conduction–convection thermosol perforated drum unit where hot air is sucked from the drum interior, thereby causing the fabric to be heated by both direct contact with the hot drum surface and by forced convection with hot air—achieving a higher rate of fabric heating.

In the infrared units the fabric is guided straight between the heating elements that can have temperatures varying from 500°C to 2000°C, depending on the desired production speed. Close control of the fabric surface temperature is important in order to avoid partial melting of the fibers at the fabric surface.[6]

Direct contact units are more susceptible to dye vapor contamination and can easily damage the fabric appearance and hand properties—especially at high temperatures (210°C). In cases where the fabric hand is important, only forced convection and infrared thermosol units are considered.

Thermosol units have distinct advantages over the previous generation of aqueous dyeing systems like jigs, winches, beam dyeing, etc. No carrier is needed during the thermosoling of polyester with disperse dyes; in addition, the fabric is processed in its full width, thereby eliminating rope marks—as in the jet or winch dyeing equipment.[7]

Whenever the term thermosol is used in this text, it is meant fixing the disperse

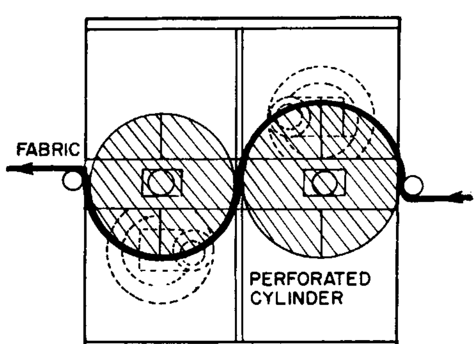

Fig. 4. Conduction–convection thermosol unit.

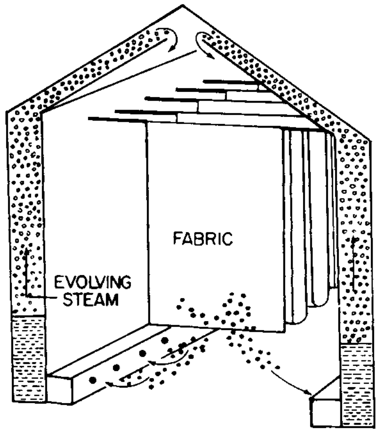

Fig. 5. Superheated steam path in high-temperature steamers.

dye into the polyester fabric by using hot air convection heating and not direct contact heating, unless specifically mentioned otherwise.

High Temperature Steaming (HT Steaming)

The high temperature steaming process came into existence after the thermosol. HT steaming was developed in the mid 1960s by ICI in England. This process makes use of superheated steam at atmospheric pressure for dye fixation.[8,9] It became very popular for the dyeing of polyester–cotton blends; it was found that the fixation of both the reactive dye (in cotton) and the disperse dye (in polyester) is improved in the presence of superheated steam compared to dry air as in thermosol.[10]

In early steamer designs, large volumetric flow rates of superheated steam at higher temperatures, well above the desired fabric temperature, were normally consumed. This was done in order to compensate for the heat loss to the surroundings and prevent condensation on the inside walls of the steaming chamber, which can cause "water drip spots" on the processed material. Modern steamers now used in industry contain open live steam lines and closed coil lines. The steamer side walls and ceiling are well insulated and maintained at a higher temperature than that of the steaming chamber. This is done by allowing the superheated steam, at a higher temperature, to run in the side walls and ceiling through closed coil lines before emerging out from open live steam lines to the steaming chamber at the required temperature, as in Figure 5. This had been found to reduce the steam consumption to about one third of that required without circulation.[11] Steamers of this type contain a water seal at the exit end, which prevents loss of steam, in addition to a continuous overflow of cold water, which eliminates dyestuff buildup in the seal.

Steamers used for the continuous thermofixation of polyester fabrics offer a fringed path to the fabric in a steam surrounding, thereby increasing the unit capacity and saving floor space, making the unit more economical to operate.

Other variations in the steamer designs are means of minimizing the tension on the fabric while travelling into the steamer, as well as providing control systems for recycling and purifying the used steam from any volatile contaminants.

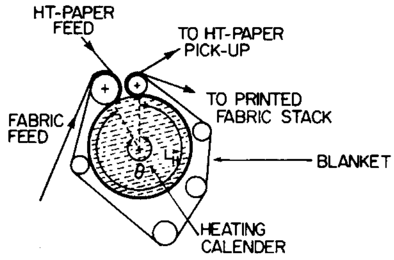

Fig. 6. Continuous heat transfer printing.

Heat Transfer Printing (HTP)

Vaporization (sublimation) transfer printing for coloring polyester with disperse dyes was first discovered in France by de Plasse.[12] This process was first adopted in industry about 1967. Thermosol and HT steaming can only be operated economically in a continuous mode, HTP can be, and is, performed continuously, batchwise, and cyclicly. Nevertheless, the principle of operation is the same: The dye is vaporized from a paper substrate while in close contact with the fabric; the dye in the vapor phase is then adsorbed and penetrates the fabric. The dye vapor coloration mechanism applies also for thermosol and HT steaming with the difference in the initial dye position: In both thermosol and HT steaming the dye particles are deposited on the fiber surface, whereas in HTP the dye particles are deposited on a separate substrate or carrier which is in conventional HTP the heat transfer paper.

In continuous HTP operation, as in Figure 6, the fabric is pressed against the heat transfer paper (HT paper) that is in contact with the hot surface (at about 210°C) of a rotating cylinder calender. For a given duration of contact heating between the HT paper and fabric, the larger the calender diameter is, the faster will be the machine production as a result of increasing the area of heat transfer between the HT-paper–fabric assembly and the surface of the calender and as expressed below:

$$L_H = v_p t = \pi d(\theta/360) \tag{1}$$

where L_H = portion of the calender circumference in contact with the fabric (m), which is directly proportional to the area of heat transfer from the calender surface to the HT paper and fabric, v_p = production velocity (m/s), t = contact time that is necessary for a differential area of the fabric (dA) to be heat-transfer printed (s), d = calender diameter (m), and θ = wrapup angle—as in Fig. 6. Assuming a typical heat transfer printing time of 20 s a production speed of 0.2 m/s, and a θ of 330°, then the required calender diameter is 1.4 m from eq. (1).

As can be seen from eq. (1), the calender diameter (d) is directly proportional to the velocity of production (v_p) for a given HTP residence time (t). Very large calenders of over 2 m in diameter offer alignment problems between the fabric, heat transfer paper, and the blanket that presses the fabric and paper against the heated calender surface. This is why the operating velocity in conventional HTP calenders is around 0.3 m/s—about one third of the possible thermosol or HT steaming production rate.

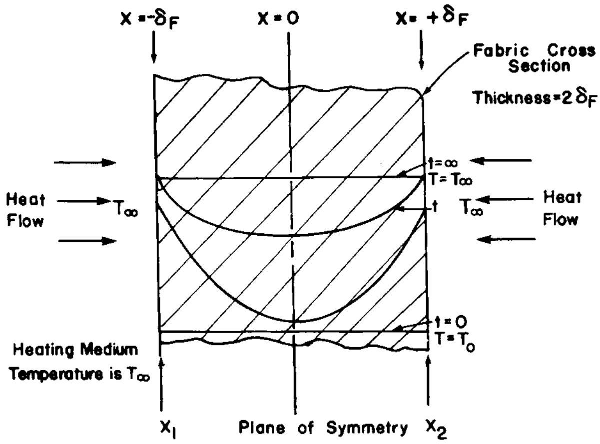

Fig. 7. One-dimensional heat transfer to a fabric: (T_0) initial fabric temperature at time (t) equal to 0, (T) fabric temperature at any time (t) and position (x) in the fabric.

Batch HTP is performed by using hot presses. The usual setup is to have the upper plate heated and pressed against the heat transfer paper and fabric. Higher production rates can be achieved by heating both the upper and lower plates, thereby reducing the time of HTP by accelerating the heating of the HTP components: fabric and paper.

In cyclic operation, the HTP is carried out by using a hot press that operates automatically: receives, say, a garment piece with the HT paper on it, prints, releases, and receives again .... The typical pressure used in HTP is about 13.8 kN/m^2 (2 psi g) at a temperature of 200°C.[7]

Like direct contact thermosol units, HTP has a relatively high rate of heating the fabric but causes dye vapor contamination problems as well as a reduction in the fabric hand properties; nonetheless, for some applications this is acceptable. As a matter of fact, HTP is becoming more and more popular for printing polyester material, and research in industry is active for extending its application to other natural and synthetic fibers.

HEAT TRANSMISSION TO THE FABRIC SYSTEM: FABRIC, FIBER, DYE PARTICLE

Fabric Heating

Figure 7 is a schematic representation of a fabric that is immersed in a heating medium of a temperature (T_∞), and is heated from both sides. For a 1-dimensional heat transfer, as in Figure 7, the mean space temperature (T_m) is

$$T_m(t) = \frac{\int_{x_1}^{x_2} T(t,x)\,dx}{(x_2 - x_1)} \tag{2}$$

where x is the heat transfer direction along which the temperature is averaged, T_m is function of time only whereas T is the function of both time and position in the x-direction. In the case of a fabric, $(x_2 - x_1)$ represents the fabric thickness $(2\delta_F)$.

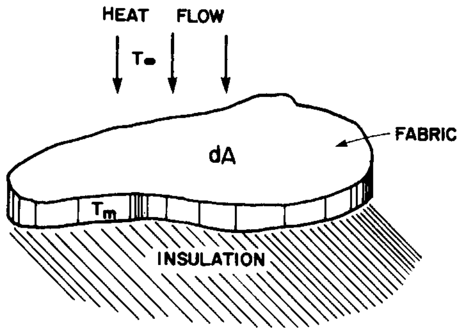

Fig. 8. Heat transmission to a fabric differential area (dA): (T_m) mean temperature of fabric as expressed in eq. (2).

The thermal analysis of a representative differential surface area (dA) of a fabric that is initially at temperature (T_0), and is (the fabric) continuously fed for a time in residence (t) within a heating unit that is constantly maintained at temperature (T_∞), can be approximated to the thermal analysis of a plate that is initially at temperature (T_0) and then is (the plate) suddenly, at ($t = 0$), immersed into a heat source having a constant temperature (T_∞)—when the differential surface area of the fabric (dA) enters the heating unit, this is like the plate being suddenly subject to the heat source.

The analysis of the heat transfer to the fabric can be made on one half of the fabric only because of the symmetry of the temperature distribution at any time t—as shown in Figure 7. The heating rate, or the change of T_m with time (dT_m/dt), in one half of the fabric cross section is a mirror image of the heating rate of the other fabric half. At the plane of symmetry, the temperature gradient is zero, i.e., ($\partial T/\partial x = 0$); therefore, no heat can hypothetically flow across the middle of the fabric. In other words, each half of the fabric is an insulation to the other fabric half. Accordingly, the heating rate of a fabric—with a thickness of ($2\delta_F$)—that is heated from both sides is simply equal to the heating rate of the same fabric—with a thickness of (δ_F)—when heated from one side while insulated from its other side.

Numerical solutions for the temperature distribution in the plate (approximation of the fabric) cross section as function of time are already available and are graphically represented for convenience.[13] Due to the fact that the fabric is a relatively thin plate and the heat transfer coefficients used to heat the fabric are relatively low, the temperature gradient inside the fabric cross section is of a few degrees during most of the heating process; hence, the fabric temperature can be assumed for the sake of simplicity to be at all times uniform and equal to the mean space temperature (T_m).

A simple expression involving the fabric mean temperature (T_m) and an overall heat transfer coefficient (h) will be derived. The fabric heating rate under a fixed temperature gradient is directly proportional to the heat transfer coefficient, which reflects the ease of the heat transmission from the heat source to the fabric. An energy balance on a fabric surface differential area (dA) that is heated from one side and insulated from the other side, as in Figure 8, during a time period (dt) (heat flow to the fabric = heat gained by the fabric), gives upon substitution

$$h_F \cdot dA \cdot (T_\infty - T_m) \cdot dt = dA \cdot \rho'_F \cdot C_F \cdot dT_m \tag{3}$$

where h_F = overall heat transfer coefficient to fabric ($W/m^2 \cdot {}^\circ K$), T_m = mean fabric temperature (°K), T_∞ = heating medium temperature (°K), dA = fabric differential surface area (m^2), t = time (s), ρ_F' = areal fabric density (kg/m^2), and C_F = fabric specific heat ($kJ/kg \cdot {}^\circ K$). Rearranging eq. (3) and integrating from ($t = 0$) to ($t = t$) and from ($T = T_0$) to ($T = T_m$) yields

$$\frac{h_F}{\rho_F' \cdot C_F} \int_{t=0}^{t=t} dt = \int_{T_m=T_0}^{T_m=T_m} \frac{dT_m}{(T_\infty - T_m)} \tag{4}$$

$$\frac{h_F \cdot t}{\rho_F' \cdot C_F} = \frac{A_F' \cdot h_F \cdot t}{C_F} = \ln \frac{(T_\infty - T_0)}{(T_\infty - T_m)} \tag{5}$$

where A_F' = specific heat transfer area of fabric heated from one side (m^2/kg). Solving eq. (5) for T_m gives

$$T_m = T_\infty - (T_\infty - T_0) \exp[-h_F \cdot t/(\rho_F' \cdot C_F)] \tag{6}$$

In this case, the areal density of the fabric (ρ_F') is also equal to the weight of fabric (kg) for every unit area (m^2) available for heat transfer—for a fabric heated from both sides, the area available for heat transfer will double and accordingly the weight of fabric per unit area of heat transfer will drop by one half:

$$A_F'' = 2/\rho_F' \tag{7}$$

where (A_F'') is the specific fabric heat transfer area (kg/m^2) when the fabric is heated from both sides or (A_F) for simplicity. Thus eq. (5) becomes

$$\frac{2 \cdot h_F \cdot t}{\rho_F' \cdot C_F} = \frac{A_F'' \cdot h_F \cdot t}{C_F} = \ln \frac{T_\infty - T_0}{T_\infty - T_m} \tag{8}$$

$$\rho_F' = \rho_F(2\delta_F) \tag{9}$$

where ρ_F = fabric density (kg/m^3) and $2\delta_F$ = fabric thickness (m). Equation (8) is the expression for the heat transfer to a fabric in a heating unit, but, due to the fact that the fabric heating rate measurements are usually made by inserting a thermocouple between two layers of fabric, and assuming that the fabric-back temperature is approximately equal to T_m, eq. (5) is commonly used to represent the fabric heating rate in the literature.[5,7]

Unsteady State Heating of a Fiber

A similar methodology can be adopted for representing the heating of a fiber, which will be useful in a later stage of this analysis. A fiber can be considered as a cylinder of an infinite length and radius (R_f), and an energy balance on a cylinder unit length during a period of time (dt) gives

$$h_f \cdot 2\pi R_f \cdot (T_\infty - T_m) \cdot dt = \pi R_f^2 \cdot \rho_f \cdot C_f \cdot dT_m \tag{10}$$

where h_f = overall heat transfer coefficient to fiber ($W/m^2 \cdot {}^\circ K$), R_f = fiber radius (m), ρ_f = fiber density (kg/m^3), C_f = fiber specific heat capacity ($kJ/kg \cdot {}^\circ K$), T_m = fiber mean temperature (°K), and

$$T_m(t) = \frac{\int_{r=0}^{r=R} T(r,t) \cdot 2\pi r \cdot dr}{\pi R_f^2} \tag{11}$$

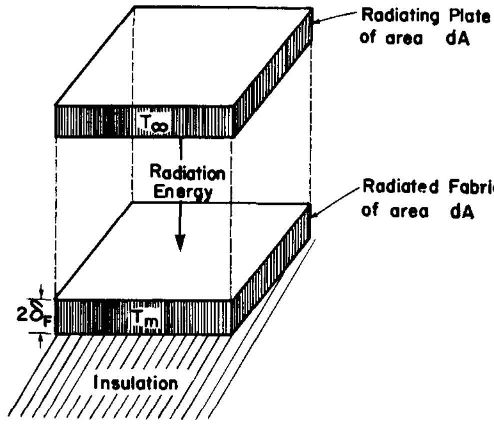

Fig. 9. Heat radiation to a fabric differential area (dA).

Integrating eq. (10) and rearranging yields

$$\frac{h_f \cdot t}{\rho_f \cdot (R_f/2) \cdot C_f} = \frac{A_f \cdot h_f \cdot t}{C_f} = \ln \frac{T_\infty - T_0}{T_\infty - T_m} \tag{12}$$

where

$$A_f = \frac{1}{\rho_f \cdot R_f/2} \tag{13}$$

A_f = specific area of heat transfer for a fiber that is heated all around (m^2/kg).

Infrared Radiation Heating of a Fabric

An expression for the infrared radiation of a fabric surface can be derived, again, from an energy balance on a fabric differential area (dA) as in Figure 9:

$$\text{heat energy flow to fabric} = \text{heat gained by fabric} \tag{14}$$

$$F \cdot E \cdot \sigma \cdot dA \cdot (T_\infty^4 - T_m^4) \cdot dt = dA \cdot \rho'_F \cdot C_F \cdot dT_m \tag{15}$$

where F = geometric factor, F = 1.0 for a fabric that has all of its heated surface fully exposed to the radiating element, E = fabric emissivity, E is about 0.94 for a fabric material,[9] σ = Stefan–Boltzman constant, $\sigma = 5.67 \times 10^{-8}$ W/m^2·°K^4, T_∞ = radiating element temperature (°K), T_m = fabric mean temperature (°K), as in eq. (2), and t = time (s). Rearranging eq. (15) and integrating

$$\frac{F \cdot E \cdot \sigma}{\rho'_F \cdot C_F} \int_{t=0}^{t=t} dt = \int_{T_m=T_0}^{T_m=T_m} \frac{dT_m}{(T_\infty^4 - T_m^4)} \tag{16}$$

$$\frac{A'_F \cdot E \cdot F \cdot \sigma}{C_F} t = \frac{F \cdot E \cdot \sigma}{\rho'_F C_F} t = \frac{1}{2T_\infty^3} \left\{ \frac{1}{2} \ln \left[\left(\frac{T_\infty + T_m}{T_\infty - T_m} \right) \Big/ \left(\frac{T_\infty + T_0}{T_\infty - T_0} \right) \right] + \tan^{-1} \frac{T_m}{T_\infty} - \tan^{-1} \frac{T_0}{T_\infty} \right\} \tag{17}$$

As can be seen from the above analysis, no heat transfer coefficient is involved in the heat transmission by radiation. Nonetheless, for the sake of comparison, dividing eq. (3) by (15) and solving for h_F yields

TABLE I
Fabric Heating Rate by Radiation

	Radiation						Convection (or direct contact) $t_{0.9}$ [c] (s), eq. (8)	
	h_R (W/m²·°K) T_m			$t_{0.9}$ [c] (s)			$T_\infty = T_{\infty R}$	$T_\infty = 210°C$
$T_{\infty R}$ [a] (°C)	210°C	20°C	$\bar{h}_R$ [b] (W/m²·°K)	Eq. (20)	Eq. (21)		$h_F = \bar{h}_R$	$h_F = \bar{h}_R$
210	23.2(1)	13.2	18.2	24.5	20.6		26.2	26.2
300	31.6	19.2	25.4	6.8	5.5		6.7	18.9
500	55	38.8	47.3	1.7	1.42		1.6	10.1
1000	173.6	142.5	158.1	0.2	0.2		0.2	3.0
2000	793.6	718.7	756.1	0.02	0.02		0.02[d]	0.62[d]

[a] $T_{\infty R}$ = radiating element temperature.
[b] $\bar{h}_R$ = arithmetic average of the radiation heat transfer coefficient h_R.
[c] T_m = 199°C.
[d] These values are purely hypothetical due to limited (h_F) values; in addition, eq. (8) cannot be used at high heat transfer coefficient values as will be shown in a later section—see Figure 10.

$$h_R = h_F = FE\sigma \frac{(T_\infty^4 - T_m^4)}{(T_\infty - T_m)} \tag{18}$$

where h_R = radiative heat transfer coefficient (W/m²·°K). As before, when the fabric is being irradiated from both sides the heating rate is doubled, as a result of doubling the specific area of heat transfer, and this can simply be accounted for by dividing the rhs of eq. (17) by a factor of 2, or letting

$$A_F'' = 2A_F' = \frac{1}{\rho_F'/2} \tag{19}$$

where A_F'' is, as before, the specific heat transfer area of a fabric being irradiated from both sides.

Thus, for heating a fabric from both sides, eq. (17) becomes

$$\frac{A_F'' \cdot F \cdot E \cdot \sigma}{C_F} \cdot t = \frac{F \cdot E \cdot \sigma}{(\rho_F'/2) \cdot C_F} \cdot t = \frac{1}{2T_\infty^3} \left\{ \frac{1}{2} \ln \left[\left(\frac{T_\infty + T_m}{T_\infty - T_m} \right) \bigg/ \left(\frac{T_\infty + T_0}{T_\infty - T_0} \right) \right] + \tan^{-1} \frac{T_m}{T_\infty} - \tan^{-1} \frac{T_0}{T_\infty} \right\} \tag{20}$$

The h_R coefficient is just for the purpose of comparing the heat transmission efficiency of heating units operating at different heating modes. Equation (18) shows that h_R will increase as the fabric temperature T_m increases. Usually, the radiating element temperature T_∞ is larger than the maximum desired fabric temperature (210°C), thereby reducing the variation in h_R—as demonstrated in columns 2 and 3 of Table I. Calculations in Table I are made by assuming the following parametric values for the fabric: $T_0 = 20°C$, $\rho_F' = 0.24$ kg/m², $C_F = 1.38$ kJ/kg·°K, $F = 1.0$, and $E = 0.94$.

A simpler form for expressing the time–temperature relation in heat transmission by radiation [as in eq. (20)] can be obtained by substituting h_F in eq. 8 by the value of h_R from eq. (18), which gives

$$t = \left(\frac{\rho_F' \cdot C_F}{2 \cdot F \cdot E \cdot \sigma} \right) \frac{\ln [(T_\infty - T_0)/(T_\infty - T_m)]}{(T_\infty^4 - T_m^4)/(T_\infty - T_m)} \tag{21}$$

Column 8 in Table I shows how fast a fabric will heat if subject to the same heat

TABLE II
Specific Heat Transfer Area for Different Body Geometries in Case of Symmetrical Heating of the Body

Body geometry	A_s (m^2/kg)	δ (m)
Semiinfinite plate (e.g., fabric of thickness $2\delta_F$)	$1/\rho\delta$	δ_F
Semiinfinite cylinder (e.g., fiber of radius R_f)	$2/\rho\delta$	R_f
Sphere (e.g., "spherical" dye particle of radius R_d)	$3/\rho\delta$	R_d

transfer coefficient as in column 4 for radiation ($h_F = \overline{h}_R$) but with the heating medium temperature (T_∞) held constant in all cases at 210°C. From the heating time values ($t_{0.9}$) in columns 7 and 8 in Table I, under the same heat transfer coefficient, the medium that has a higher temperature (T_∞) will always heat the fabric faster; however, higher heat source temperatures (over 210°C) may result in the melting of the "standing out" fibers at the fabric surface—see the section after the next one.

A General Expression for Heat Transmission to a Body

From Table I, it is clear that, within the range of practical accuracy of temperature and timing control, eqs. (20), (21), and (8) give similar results; thus eq. (8) can be used to express the heating of a fabric (or fiber) under all modes of heating, and h_F in eq. (8) is practically an overall heat transfer coefficient for convection, conduction, and radiation. Small deviations occur when eq. (8) is used to express heat transmission by radiation at fabric temperatures close to the radiating element temperatures, but most industrial radiating equipment has heating element temperatures well above the maximum desired fabric temperature. Thus, eq. (8) can be rewritten as

$$\frac{A_s \cdot h_T \cdot t}{C_T} = \ln\frac{T_\infty - T_0}{T_\infty - T_m} \tag{22}$$

where h_T is the overall heat transfer coefficient for all heating modes from the heat source(s) to the body that is also denoted h for simplicity, C_T is the body heat capacity, and A_s is the body specific heat transfer area. The specific area of heat transfer A_s varies in eq. (22) according to the body geometry as in Table II.

From Table II, the specific heat transfer area for the three basic geometries can be generally expressed as

$$A_s = m/\rho\delta \tag{23}$$

Accordingly, eq. (22) becomes

$$\frac{m \cdot h_T \cdot t}{\rho \cdot \delta \cdot C_T} = \ln\frac{T_\infty - T_0}{T_\infty - T_m} \tag{24}$$

where $m = 1$ for the plate, 2 for the cylinder, and 3 for the sphere—as in Table II.

Generally speaking, the resistance to the heat flow is the reciprocal value of h_T, and $h_T = h_{cv} + h_{cd} + h_R$; the heat transfer coefficients due to convection, conduction, and radiation, respectively.

TABLE III
"Standing-Out" Fiber and Fabric Heating Rates[a]

T_∞ (°C)	h_T (W/m²·°K)	$t_{0.9}$[b] (s) (T_m = 199°C) $(t_{0.9})_f$ "Standing out" fiber in fabric	$(t_{0.9})_F$ fabric	$(T_m)_F$ (°C) Mean fabric temperature after a duration of $(t_{0.9})_f$ (s)
210	1.16	28.7	411.6	
	11.60	2.9	41.2	55
	116.00	0.3	4.1	
500	1.16	4.65	66.8	
	11.60	0.5	6.7	35
	116.00	0.05	0.7	
1000	1.16	2	28.8	
	11.60	0.2	2.9	33.6
	116.00	0.02	0.3	

[a] Using eq. (24).
[b] $t_{0.9}$ = time (s) for T_m to reach 199°C. Values used for the above computations are: $R_f = 10^{-5}$ m, $\rho_f = 1.38 \times 10^3$ kg/m³, C_f = 1.67 kJ/kg·°K, ρ_F' = 0.24 kg/m², and C_F = 1.38 kJ/kg·°K.

Heating Rate of "Standing Out" Fibers at Fabric Surface

Table III shows the "standing out" fiber (at the fabric surface) heating rate for reaching a mean temperature T_m of 199°C under different heat transfer coefficients and heat source temperatures.

In cases where more uniform heating of the fabric cross section is required, higher heating medium temperatures cannot be used even at lower heat transfer coefficients, as demonstrated in column 5 of Table III. Lower heating medium temperatures (and lower heat transfer coefficients) result in less difference between the fabric surface "standing-out" fiber temperature and fabric bulk temperature.

On the other hand, if it is desired to only heat the fabric surface, then the higher the medium temperature (T_∞), the larger the temperature difference between the fabric surface and the fabric bulk. However, a diminishing return does exist, for instance, by increasing (T_∞) from 210°C to 500°C the temperature difference between the fiber at the fabric surface and the fabric bulk increases by 20°C (from 55°C to 35°C), but by increasing the heating source temperature to 1000°C the temperature difference is only increased by 1.4°C—as in column 5 in Table III.

By dividing eq. (8) by eq. (12) one obtains the fabric "standing-out fiber" heating time ratio (t_F/t_f) for reaching the same temperature T_m:

$$\frac{t_F}{t_f} = \left(\frac{C_F}{C_f}\right) \cdot \left(\frac{A_f h_f}{A_F h_F}\right) \tag{25}$$

Substituting from eqs. (7) and (13) for the values of A_f and A_F as in Table II gives

$$\frac{t_F}{t_f} = \left(\frac{C_F}{C_f}\right) \cdot \frac{[2/(\rho_f \cdot R_f] \cdot h_f}{[1/(\rho_F \cdot \delta_F)] \cdot h_F} \tag{26}$$

For the values used in the computations for Table III one obtains

$$\frac{t_F}{t_f} = \left(\frac{1.38}{1.67}\right) \cdot \frac{[2/(1380 \times 10^{-5})]}{[1/(240 \times 0.0005)]} \cdot \frac{h_f}{h_F} = 14.35 \left(\frac{h_f}{h_F}\right) \tag{27}$$

which explains the 14 times faster heating rates of the fiber at the fabric surface compared to the fabric bulk in Table III. (In Table III it was assumed for the sake of simplicity that $h_f = h_F$.) The thicker and heavier the fabric is, the larger will be the value of (ρ'_F) in eq. (26), and the faster will heat the "standing-out" fibers compared to the bulk of the fabric. The specific heat transfer ratio (A_f/A_F), in eq. (25), indicates that the specific surface area prevailing for heat transfer to a fiber is about 14 times larger than that of the fabric.

Dye Particle Heating

Equations similar to eq. (25) provide very useful correlations for estimating the relative heating time of substances having different shapes and/or structures, when subject to the same heating source temperature.

For example, one can estimate the heating time of "spherical" disperse dye particles deposited on the fiber surface and having a radius (R_d) of 10^{-6} m (1 μ) and a density (ρ_d) of 1.0×10^3 kg/m^3. The specific area of heat transfer of a sphere subject to the heat source from all around is as in Table II, $A_d = 3/\rho_d \cdot R_d$, and for the fiber, $A_f = 2/\rho_f \cdot R_f$; thus, substituting as in eq. (25) yields

$$\frac{t_f}{t_d} = \frac{(C_f/h_f)}{(C_d/h_d)} \cdot \left(\frac{A_d}{A_f}\right) \quad \text{and} \quad \frac{A_d}{A_f} = \frac{(3/\rho_d \cdot R_d)}{(2/\rho_f \cdot R_f)} = \frac{(3/1000 \times 10^{-6})}{(2/1380 \times 10^{-5})} = 20.7 \tag{27'}$$

Assuming that both the fiber and the dye particles have the same heat transfer coefficients and that, for the sake of argument, the heat capacity of both materials is comparable, then from the above calculation the dye particle will heat about 20 times faster than the fiber. No data could be found in literature on disperse dye heat capacity. Such data is normally obtained under low heating rate conditions. Heat capacity measurements under high heating rate conditions, as prevailing during the continuous processes under investigation, are difficult to obtain and would produce a spectrum of apparent values. The C_d value assumed in this section is of the same order of magnitude as the heat capacity of similar solid material found in Ref. 13.

As the dye particle sublimes and the particle "radius" vanishes, the ratio A_d/A_f approaches infinity and the dye particle rate of heating relative to the fiber accelerates.

In fabric printing, the dye particle is part of a porous film and heats according to the film heating rate.

Limitations of the General Expression for Fabric Heating

Equation (24) is very useful for expressing solid body heating cases where the temperature distribution inside the body can be approximated by a uniform and mean temperature (T_m), that is, in cases where small temperature gradients exist between the body center and surface. This approximation can be offset by high temperature gradients between the body surface and center by either increasing the heat transfer coefficient, or in cases where the distance between the body surface and center is large. But since eq. (24) is being used on fabrics, fibers, and dye particles of relatively small dimensions in the direction of the heat flow (or large specific heat transfer surface areas as in Table II), the main equation limitation is its inadequacy for heating conditions involving high heat transfer coefficient values—as the ones in Table I for high radiating element temperatures. Under such circumstances the temperature distribution inside the body is far from uniform and T_m cannot be calculated from Eq. (24).

According to eq. (24), as h_T approaches infinity, t will go to zero, and $T_m \rightarrow T_\infty$ in no time. This does not happen in reality; the heat transmission through the fabric thickness (as $h_T \rightarrow \infty$) becomes limited by the fabric thermal diffusivity.

When analyzing the heat transport between different phases, two sets of variables have to be considered: the thermal diffusivity of each phase and the heat transfer coefficients between phases. The thermal diffusivity reflects the capacity within the phase for thermal diffusion. The heat transfer coefficient between two phases is an indication of the ease with which heat flows from one phase to the other, or the interface capability for heat transfer.

Let us first consider the case when $h_T = \infty$ and heat is transferred to the fabric through a perfect contact between the heat source and the body interface, i.e., at $t \geqslant 0$, the fabric surface temperature equals the heat source temperature (T_∞).

The transient 1-dimensional heat conduction in a homogeneous medium can be expressed by the following differential equation:

$$\frac{\partial T}{\partial t} = \alpha_F \frac{\partial^2 T}{\partial x^2} \tag{28}$$

where T = fabric temperature (°K), when assuming the fabric to be a homogeneous plate—as in Figure 7—t = time (s), α_F = fabric thermal diffusivity (m²/s), x = distance along the fabric thickness (m) in the direction of the heat transfer (see Fig. 7).

$$\alpha_F = \frac{k_F}{\rho_F C_F} \tag{29}$$

where k_F = fabric thermal conductivity (W/m·°K), ρ_F = fabric density (kg/m³), and C_F = fabric specific heat capacity (kJ/kg·°K).

Measurements for the variation of k_F and C_F for a jersey knitted fabric had been made.[14] In the temperature range 20–200°C, C_F varies from 1.05 to 1.67 (kJ/kg·°K) and k_F varies from 0.06 to 0.066 (W/m·°K); the changes in C_F and k_F in the investigated temperature range are almost linear. In order to simplify the thermal analysis, the values of the system physical properties (especially when their variations with temperature are small) are taken at the arithmetic average temperature, which is in our case 110°C; thus, k_F = 0.064 W/m·°K and C_F = 1.38 kJ/kg·°K. Thus, for a fabric having ρ'_F = 0.24 kg/m² and $2\delta_F$ = 0.001 m,

$$\alpha_F = \frac{0.064}{(0.24/0.001) \times 1380} = 1.93 \cdot 10^{-7}\ \mathrm{m^2/s} \cong 2 \times 10^{-7}\ \mathrm{m^2/s} \tag{30}$$

For the initial, boundary, and final conditions (see Fig. 7),

$$\text{at } t < 0, \quad T = T_0 \quad \text{at } -\delta_F \leqslant x \leqslant +\delta_F \tag{31a}$$

TABLE IV
Comparison between the Fabric Heating Rate Solutions Obtained Using eq. (24) and Numerical Analysis

	$t_{0.9}$ (s) (T_m = 199°C)	
h_T (W/m^2·°K)	Numerical analysis[13]	Eq. (24)
0	∞	∞
40	12.0	12.0
58	9.0	8.2
93	6.1	5.1
116	5.2	4.1
232	3.3	2.1
465	2.2	1.0
697	1.9	0.7
930	1.7	0.5
1160	1.6	0.4
2320	1.5	0.21
∞	1.37	0.0

$$\text{at } t \geqslant 0, \quad T = T_\infty \quad \text{at } x = \pm\delta_F \tag{31b}$$

$$\text{at } t = \infty, \quad T = T_\infty \quad \text{at } -\delta_F \leqslant x \leqslant +\delta_F \tag{31c}$$

where T_0 is the initial fabric temperature (20°C) and (T_∞) is the heating source temperature (210°C), eq. 28 can be solved by the separation of variables,[15] which gives

$$\frac{T_\infty - T}{T_\infty - T_0} = 4 \sum_{n=0}^{n=\infty} \frac{(-1)^n}{(2n+1)\cdot\pi} \exp[-(2n+1)^2 \cdot \pi^2 \cdot \alpha_F \cdot t/(4 \cdot \delta_F^2)] \cdot \cos\left[(2n+1)\cdot\frac{\pi \cdot x}{2\delta_F}\right] \tag{32}$$

The mean fabric temperature (T_m) can be obtained by substituting for T from eq. (32) in eq. (2), which yields upon integration and arrangement eq. (33):

$$\frac{T_\infty - T_m}{T_\infty - T_0} = 8 \sum_{n=0}^{n=\infty} \frac{\exp[-(2n+1)^2 \cdot \pi^2 \cdot \alpha_F\, t/(4 \cdot \delta_F^2)]}{(2n+1)^2 \cdot \pi^2} \tag{33}$$

Fortunately, eq. (33) converges very rapidly for relatively long heating times. For example, for t = 1 s, eq. (33) gives

$$\frac{T_\infty - T_m}{T_\infty - T_0} = 8\,[1.4075 \times 10^{-2} + 2.1682 \times 10^{-10} + 1.5 \times 10^{-24} + \cdots] = 0.1126 \tag{34}$$

Therefore, T_m = 188.6°C after 1 s (t = 1 s) for the fabric in question, and for $t \doteq 0.5$ s

$$\frac{T_\infty - T_m}{T_\infty - T_0} = 8\,(3.776 \times 10^{-2} + 1.562 \times 10^{-6} + 7798 \times 10^{-14} + \cdots) \tag{35}$$

Therefore, T_m = 152.6°C after 0.5 s.

Equations (34) and (35) show how the convergence of the infinite series in eq. (33) is slowed down by decreasing the time (t), e.g., for t = 0.1 s, the second term in the series becomes 1.9051×10^{-3} compared to 2.1682×10^{-10} when t = 1.0 s.

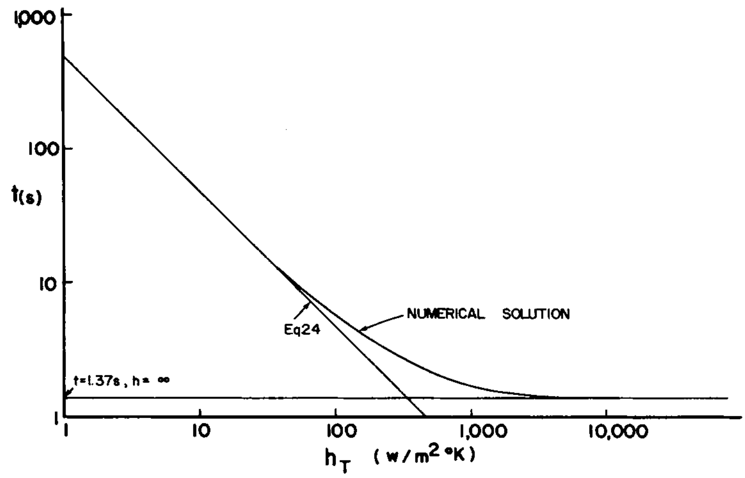

Fig. 10. Effect of the heat transfer coefficient on the fabric heating time ($t_{0.9}$) and comparison between results obtained from numerical analysis[13] and eq. (24).

Thus for the particular fabric under investigation and for heating times over 0.5 s one can safely approximate eq. (33) by neglecting all terms in the series except the first term, which yields

$$\frac{T_\infty - T_m}{T_\infty - T_0} \cong \frac{8}{\pi^2} \cdot \exp\left(-\pi^2 \cdot \frac{\alpha_F}{4 \cdot \delta_F^2} \cdot t\right) \quad \text{for t} \geqslant 0.5 \text{ (s)} \tag{36}$$

From eq. 36 ($h = \infty$) and for $T_\infty = 210°C$, the time necessary for (T_m) to reach 199°C is $t = 1.36$ s, which is the shortest possible time for heating the fabric, whereas from eq. (24) with $h_T = 1162$ W/m^2·°K, $t = 0.4$ s. The difference between the heating times 0.4 s and 1.36 s as obtained from the exact solution [eq. (36)], and the simple heat transfer model [eq. 24] demonstrates the limits of eq. (24). Graphical representations of eqs. (32) and (33) are available and are more convenient to use.[13,15,16]

Numerical Solution and General Expression for Fabric Heating—A Comparative Analysis

A comparison between values of $t_{0.9}$ ($T_m = 199°C$) using available graphical solutions of the numerical analysis[13] for the boundary conditions as in eqs. (31a), (31b), and (31c) and values of ($t_{0.9}$) obtained from eq. (24) are shown in Table IV for different values of h_T. Nevertheless, for most practical purposes the heat transfer coefficient of industrial heating units for fabrics seldom exceeds a few hundred W/m^2·°K as will be shown later.

Table IV shows the diminishing return of increasing the heat transfer coefficient. Increasing h_T from 93 to 232 W/m^2·°K cuts the necessary heating time ($t_{0.9}$) by about one half from 6.1 to 3.3 s, beyond that h_T needs to be increased by an order of magnitude (232–2320) in order to reduce $t_{0.9}$ by another 50%. Figure 10 illustrates the results obtained in Table IV and the deviation of eq. (24) from the numerical analysis solution at high heat transfer coefficient values. Figure 10 also shows how trying to increase h_T over 400 (W/m^2·°K) produces an insignificant effect on the speed of heating the fabric.

The textile literature should recognize the limitations of eq. (24) in order to avoid serious errors in estimating the overall heat transfer coefficient of heating processes involving high h_T values—as in HTP—as will be demonstrated in Paper II of this study.

SUMMARY

In this investigation, first, the three common processes for continuously coloring polyester with disperse dyes are briefly reviewed, and the slower production rate of the conventional HTP relative to thermosol or HT steaming is simply analyzed [eq. (1)]. Then a general expression that represents the heat transmission by conduction, convection, and/or radiation to the fabric system components (fabric, fiber, dye particle) is derived [eq. (22)]. Next, a methodology for estimating the relative heating rate of the different fabric components is used to demonstrate that, for the typical polyester fabric under investigation, the fibers standing out at the fabric surface heat up about 14 times faster than the fabric bulk [eq. (27)], which explains the necessary close control of the fabric surface temperature when using infrared thermosol units containing high temperature heating elements in order to avoid partial melting of the fabric surface. The same methodology is also used to show that a dye particle (of 2×10^{-6} m in diameter) heats up about 20 times faster than the polyester fiber (2×10^{-5} m in diameter) it is deposited upon [eq. (27′)]. Finally, the limitations of the general heat transmission [eq. (22)] are investigated for the fabric heating. For the fabric under investigation, results obtained from eq. 22 for the heating time for the fabric to reach 200°C ($t_{0.9}$) start deviating from the results obtained from the numerical analysis solution[13] (by approximating the fabric to a homogeneous plate) for heat transfer coefficient values over 40 (W/m^2·°K); as in Figure 10. Under such circumstances the uniform temperature distribution inside the body being heated—a basic assumption for eq. (22)—is violated. In the case of the fiber and dye particle, the body geometry is so small such that increasing the heat transfer coefficient (up to, say, 200 W/m^2·°K) does not significantly affect the body temperature distribution uniformity. If eq. (22) is used for high heat transfer coefficients to represent the heating rate of a fabric, it will yield heating times shorter than those obtained from the more exact numerical analysis—as in Table IV.

References

1. P. Richter, "Efficient High-Temperature Dyeing of Polyester Fibers—Principles and Practical Experience," Rapid Dyeing Conferences, Shirley Institute Publication S31, Manchester, England, 1977, p. 19.

2. J. Gibson, U.S. Pat. 2,663,612 (1953).

3. J. J. Iannarone and W. J. Wygand, "Dyeing Blends of Dacron Polyester Fiber and Cotton by the DuPont Thermosol Process," *Am. Dyestuff Rep.*, **49,** 82 (1960).

4. V. Tullio, "Thermosol Dyeing of Polyester–Cotton Blends," *Am. Dyestuff Rep.*, **55,** 412 (1966).

5. H. Hauben and M. Pabst, "Thermosolage et Thermofixation sur les Machines a Cylindres," *Teintex*, No. 10, 519 (1974).

6. W. J. Wygand, "The Continuous Dyeing of Blends of Polyester Fibers and Cotton," *Am. Dyestuff Rep.*, **53,** 1066 (1964).

7. E. J. Gorondy, "Vapor Fixation of Disperse Dyes in Polyester," AATCC International Dyeing Symposium on Practical Dyeing Problems. Analysis and Solutions, Washington, D.C., May 25–26, 1977, p. 75.

8. A. P. Lockett, "Some Possibilities of High-Temperature Steaming in Textile Printing," *J. Soc. Dyers Colourists*, **83,** 213 (1967).

9. M. R. Fox, W. J. Marshall, and N. D. Stewart, "Padding, Drying, Steaming and Baking Stages in the Application of Dyes to Cellulose Fibers and their Blends with Polyester Fibers," *J. Soc. Dyers Colourists*, **83,** 493 (1967).

10. R. T. Norris, "High Temperature Steaming in Continuous Piece Goods Dyeing," *Text. Chem. Colorists*, **1,** 88 (1969).

11. L. W. C. Miles, "Dye Fixation with Steam," *Ciba-Geigy Rev.*, No. 2, 18 (1974).

12. N. de Plasse, F. R. Pat. 1,223,330 (1948).

13. C. P. Kothandaraman and S. Subramanyan, *Heat and Mass Transfer Data Book*, 2nd ed., Wiley, New York, 1975.

14. S. Baker, G. C. Tesoro, T. Y. Toong, and N. A. Moussa, *Textile Fabric Flammability*, MIT Press, Cambridge, Mass., 1976.

15. R. B. Bird, W. E. Stewart, and E. N. Lightfoot, *Transport Phenomena*, Wiley, New York, 1960, p. 243.

16. R. H. Perry and C. H. Chilton, *Chemical Engineering Handbook*, 5th ed., McGraw-Hill, New York, 1973.

Received October 9, 1981
Accepted June 24, 1982